Elsevier Editorial System(tm) for Industrial Crops and Products

Manuscript Draft

Manuscript Number:

Title: Production and characterization of PLA_PBS biodegradable blends reinforced with cellulose nanocrystals extracted from hemp fibres

Article Type: SI: Nanocellulose

Keywords: Poly(lactic acid), poly(butylene succinate), blend, cellulose nanocrystals, hemp, compost.

Corresponding Author: Dr. Elena Fortunati, Ph.D.

Corresponding Author's Institution: University of Perugia

First Author: Francesca Luzi, PhD student

Order of Authors: Francesca Luzi, PhD student; Elena Fortunati, Ph.D.; Alberto Jiménez, PhD; Debora Puglia, PhD; Daniela Pezzolla, PhD; Giovanni Gigliotti, Prof; Josè M Kenny, Prof; Amparo Chiralt, Prof; Luigi Torre, Prof

Abstract: Poly(lactic acid) (PLA) and poly(butylene succinate) (PBS) were blended and bionanocomposite films were prepared by solvent casting method adding 1 or 3 %wt of cellulose nanocrystals extracted from Carmagnola carded hemp fibres. Both unmodified (CNC) and surfactant modified (s-CNC) cellulose nanocrystals were loaded to PLA matrix or to PLA_PBS blend in order to produce binary or ternary formulations while the thermal, morphological, mechanical, optical and barrier properties of all the produced systems were deeply investigated. Mechanical analysis showed increased values of Young's modulus in binary and ternary formulations, more evident in the CNC based formulations. The presence of both CNC and s-CNC and the addition of PBS to PLA matrix provoked an improvement of barrier properties. This behaviour could be related to the synergic ability of cellulose nanocrystals to increase the tortuous path of gas molecules with the increase in the crystallinity degree induced by the presence of PBS. The disintegration in composting conditions of different PLA and PLA_PBS based bionanocomposites was also investigated. The results showed that all the formulations disintegrated in less than 17 day while s-CNC were able to promote the disintegration behaviour although the PBS presence obstacles the disintegrability. During the composting, the main chemical parameters were investigated in order to assess changes in the composition of the tested mixtures. The organic matter (OM) loss occurred in both control and in the PBS_PLA based bionanocomposites composts in the 90 days of treatment. Neverthless the total organic C content showed values >20; moreover a low concentrations in heavy metal in both composts as recomended by the Italian and European law were observed.

Suggested Reviewers: ARANTZAZU VALDES GARCIA
arancha.valdes@ua.es

Marina Ramos
marina.ramos@ua.es

Giovanna Buonocore
gbuonoco@unina.it

Fabrizio Sarasini
fabrizio.sarasini@uniroma1.it

Liliana Manfredi
lbmanfre@fi.mdp.edu.ar

Highlights (for review)

- Cellulose nanocrystals (CNC) were isolated from *Carmagnola* carded hemp fibres.
- The surface of nanocrystals was also modified using a commercial surfactant (s-CNC).
- PLA and PLA_PBS nanocomposites reinforced with CNC and s-CNC were developed.
- CNC, s-CNC and PBS provoked an increase of PLA barrier and mechanical properties.
- All the formulations disintegrated in less than 17 days in composting conditions.

Production and characterization of PLA_PBS biodegradable blends reinforced with cellulose nanocrystals extracted from hemp fibres

F. Luzi[a], E. Fortunati[a1], A. Jiménez[b], D. Puglia[a], D. Pezzolla[a], G. Gigliotti[a], J. M. Kenny[a], A. Chiralt[b], L. Torre[a]

[a]*University of Perugia, Civil and Environmental Engineering Department, UdR INSTM, Strada di Pentima 4, 05100 Terni (Italy)*
[b]*Instituto Universitario de Ingeniería de Alimentos para el Desarrollo, Universitat Politècnica de València, Camino de Vera s/n, 46022 Valencia, Spain.*

[1]**Corresponding author:** Tel.: +39-0744492921; fax: +39-0744492950; E-mail address: elena.fortunati@unipg.it (E. Fortunati)

Abstract

Poly(lactic acid) (PLA) and poly(butylene succinate) (PBS) were blended and bionanocomposite films were prepared by solvent casting method adding 1 or 3 %wt of cellulose nanocrystals extracted from *Carmagnola* carded hemp fibres. Both unmodified (CNC) and surfactant modified (s-CNC) cellulose nanocrystals were loaded to PLA matrix or to PLA_PBS blend in order to produce binary or ternary formulations while the thermal, morphological, mechanical, optical and barrier properties of all the produced systems were deeply investigated. Mechanical analysis showed increased values of Young's modulus in binary and ternary formulations, more evident in the CNC based formulations. The presence of both CNC and s-CNC and the addition of PBS to PLA matrix provoked an improvement of barrier properties. This behaviour could be related to the synergic ability of cellulose nanocrystals to increase the tortuous path of gas molecules with the increase in the crystallinity degree induced by the presence of PBS. The disintegration in composting conditions of different PLA and PLA_PBS based bionanocomposites was also investigated. The results showed that all the formulations disintegrated in less than 17 day while s-CNC were able to promote the disintegration behaviour although the PBS presence obstacles the

disintegrability. During the composting, the main chemical parameters were investigated in order to assess changes in the composition of the tested mixtures. The organic matter (OM) loss occurred in both control and in the PBS_PLA based bionanocomposites composts in the 90 days of treatment. Neverthless the total organic C content showed values >20; moreover a low concentrations in heavy metal in both composts as recomended by the Italian and European law were observed.

Keywords: Poly(lactic acid), poly(butylene succinate), blend, cellulose nanocrystals, hemp, bionanocomposites, compost.

1. Introduction

In the last few years, the growing concern on the environmental pollution due to the high impact of plastic wastes, has attracted the interest of academic and industrial researchers to develop green polymers extracted from natural resources. In this context, biodegradable and biocompatible polymers have received much attention respect to non-degradable polymers based on petroleum sources. Green polymer represent a valid alternative to develop new eco-friendly materials able to reduce both the plastic wastes accumulated every days in landfills and the emission of greenhouses gases, depending on fossil resources that form during the production and the disposal of the end-life (Peelman et al., 2013). Moreover, biodegradable polymers are susceptible to microbial and fungal attacks (Peelman et al., 2013; Stloukal et al., 2015); the compostable plastics are metabolized by naturally organisms with non-negative environmental impact.(Stloukal et al., 2015) The valid strategy to reduce the waste and the environmental pollution has oriented the academic researches to develop new compostable and biodegradable fresh food packaging solutions. The packaging materials, in fact, represent the higher cause of environmental pollution. Furthermore, in a more heterogeneous concept of packaging materials, the function of food packing is not only to contain and protect from external abiotic and biotic factors the products during the transportation and the

54 storage, but also to increase the shelf-life maintaining the quality and the safety of the foodstuff
55 (Rhim et al., 2013).
56 In this scenario, poly(lactic acid) (PLA) thermoplastic polymer, derived from renewable resources,
57 has been received a lot of attention than other polyesters (Lu et al., 2013; Wei et al., 2012). PLA is
58 a linear aliphatic polyester, biodegradable and compostable (Chaiwutthinan et al., 2015). PLA is
59 produced by the fermentations of renewable feedstock as starch, plant crops and sugar (Fortunati, et
60 al., 2015) and it shows a good and favourable functional properties that promote its use to infood
61 packaging. PLA is transparent, easy to process, non-toxic or carcinogenetic, economically feasible,
62 approved by US Food and Drug Administration (FDA) as a food contact substance and it is used to
63 produce packaging for short shelf-life applications. (Arrieta et al., 2013). Unfortunately, PLA
64 suffers the limitations when a comparison of the biodegradable polymer with the equivalent
65 petroleum based matrices used in food packaging applications has done. PLA is characterized by
66 poor thermal, mechanical (Arrieta et al., 2013) and gas barrier properties (water vapour and oxygen
67 permeability) necessary in the fresh food packaging to guarantee the shelf-life of the products.
68 There are many food products sensitive to water moisture and oxidation, that should be reduced
69 during the transport and the storage (Arrieta et al., 2014). In order to reduce these limitations,
70 several strategies can be adopted to modify the limited properties as previously adopted by author
71 researchers (Arrieta et al., 2014; Fortunati et al., 2014; Herrera et. 2015)
72 Therefore, the development of polymeric blend and nanocomposistes reinforced (Duncan, 2011)
73 with natural nanofillers may be necessary to provide a solution to these limitations as a valid
74 strategy to increase and modulate the properties without affecting their positive characteristics.
75 Furthermore, the aspect and the quality of the food packaging could influence the purchase of
76 consumers; for this reason high transparency in the food applications is considered an important
77 characteristic (Rhim et al., 2013). In this study, poly(butylene succinate) (PBS) was selected as a
78 valid polymer for the realization of blend based systems. PLA blended with another biodegradable

79 polymer, offers improved properties without compromising its eco-friendly and suitable
80 characteristics. PBS is chemically synthesized from bio-based renewable monomers produced by
81 the polycondensation reaction of 1,4-butanediol with succinic acid and a synthetic aliphatic
82 polyester (Bhatia et al. 2012; Chen et al., 2014), or prepared by biological fermentation process
83 from the agricultural crops containing cellulose, lactose and glucose (Hwang et al. 2012; Lin et al.
84 2015). PBS is easy to process and has high thermal, chemical resistance and good mechanical
85 properties, in particular excellent impact strength and flexibility (Bhatia et al. 2012).
86 The use of nanocomposite approach could represent an alternative to blend strategy or could be
87 combined to increase and modulate, with interesting results, the final properties required for the
88 packaging.
89 Recently, cellulose nanocrystals (CNC) have been investigated as nanoreinforcement that could be
90 used in biodegradable polymer able to improve and modulate the properties of a biomaterial for
91 food packaging applications (Arrieta et al., 2014; El-Wakil et al., 2015; Fortunati et al., 2013; Khan
92 et al., 2012; Šturcová et al., 2005). Moreover, CNC present low density, high stiffness and excellent
93 biocompatibility (Fernandes et al. 2013; Lin, Dufresne, 2014). CNC can be extracted from different
94 natural resources (Fortunati et. al., 2013; Hsieh, 2013; Luzi et al., 2014; Neto et al., 2013; Silvério
95 et al.,2013) and their dimensions depend on the raw material utilized for the extraction (Lin,
96 Dufresne, 2014) and the intensity of the chemical process selected for their production (Cranston,
97 Gray, 2006). CNC are usually characterized by rigid rod monocrystalline domains (Silvério et al.
98 2013) with diameters ranging from 1-100 nm and from ten to hundreds of nm in length (Matos et
99 al., 2000), an aspect ratio (diameter/length) that can vary from 1:1 to 1:100 and an elastic modulus
100 of around 150 GPa (Saïd Azizi Samir et al., 2004).
101 In this research, cellulose nanocrystals extracted from *Carmagnola* carded hemp fibres have been
102 used as reinforcement phases for both PLA neat matrix and PLA_PBS blends. *Carmagnola* hemp
103 plant originates from Piedmont region in Italy and it is composed from about 70% of total weight

by alpha-cellulose and hemicellulose, 44 % and 25 %, respectively (Gandolfi et al., 2013). Luzi et al. 2014 previously reported about the chemical pretreatment and CNC extraction procedure from carded hemp fibres.

Moreover, it was largely investigated the degradation of polymeric materials and the role of microorganisms in their decomposition during composting (Torres et al., 1996; Itävaara et al., 2002; Kale et al., 2007; Sangwan and Wu, 2008; Saadi et al., 2012; Karamanlioglu et al. 2014). It is well known that the composting process is strictly dependent by the environmental conditions that affect the aerobic process (i.e. relative humidity, pH, O_2, C/N ratio, temperature) and then the compostability of plastic. In addition, the rate of degradation depends on the crystallinity of the PLA (Auras et al., 2004; Kale et al., 2007).

The aim of this research is the development and characterizations of biodegradable PLA blend and bionanocomposites films for food packaging applications. Initially, the different ratio of PLA_PBS (90:10, 80:20 and 70:30, respectively) blends was optimized in terms of thermal, mechanical and morphological characteristics. Then the optimized formulation was selected to produce the PLA_PBS films reinforced with cellulose based structures. The idea was to evaluate also the effect of unmodified (CNC) and surfactant modified (s-CNC) cellulose nanocrystals in both binary PLA based film and PLA_PBS based blend. The produced formulations were fully characterized by the study of thermal, mechanical and morphological properties. Moreover, some functional properties such as optical and barrier properties were studied to evaluate the influence of CNC or s-CNC and the presence of PBS into PLA matrix. Finally, the disintegrability in composting conditions of PLA and PLA_PBS binary and ternary bionanocomposites was investigated in order to evaluate the post-use behaviour of these potential food packaging systems. As the quality of compost obtained from PLA and PBS was not deeply investigated, in this experiment was studied how the chemical parameters change during the composting as well as the quality of the produced compost.

Moreover, to confirm the effectiveness of composting process, organic matter (OM) loss, C/N ratio and a seed bioassay were measured throughout the process.

2. Experimental section

2.1 Materials

Poly(lactic acid) (PLA) 3051D, with a specific gravity of 1.25 g cm^{-3}, a molecular weight (M_n) of ca. 1.42 x10^4 g mol^{-1}, and a melt flow index (MFI) of 7.75 g 10 min^{-1} (210 °C, 2.16 kg) was supplied by NatureWorks®, USA.

Poly(butilene succinate) (PBS) was supplied by Showa Denko K.K. (Bionolle 1001MD) with a specific gravity of 1.26 g cm^{-3}.

Hemp (*Carmagnola*) pristine fibres were obtained from Assocanapa in *Carmagnola*, Piedmont, Italy. The preparation of the cellulose nanocrystals (CNC) extracted from carded hemp was previously described (Luzi et al., 2014). Cellulose nanocrystals were extracted in two steps (Figure 1, Panel A). The first step, a chemical alkali treatment, leads to remove the waxes and lignin components obtaining holocellulose materials, while the subsequent sulphuric acid hydrolysis process allows obtaining cellulose nanocrystals in an aqueous suspension. The mean diameter of the unbleached fibres was (19±3) μm, however, after chemical pre-treatments, as a consequence of elimination of waxes and lignin, the fibres appeared separated, individualized and the mean diameter reduced at about (15±4) μm. The morphological investigation of cellulose nanocrystals by a transmission electron microscope (TEM) showed that CNC were characterized by acicular rod shape structure typically of cellulose nanocrystals, (160±20) nm in length a diameter of (4.5±1) nm with an aspect/ratio of 35 (Luzi et al., 2014).

All chemical reagents were supplied by Sigma Aldrich®.

2.2 Cellulose nanocrystal modification

153 Cellulose nanocrystals extracted from hemp fibres were modified with an acid phosphate ester of
154 ethoxylatednonylphenol surfactant, (Beycostat A B09 - CECCA S.A.) (Heux et al., 2000). The use
155 of surfactant permits a physical modification of cellulose nanocrystals, since it is able to improve
156 and increase the dispersion of the CNC in the polymer matrix. The modified cellulose nanocrystals
157 (s-CNC) were prepared adding the surfactant in the proportion of 1/4 (wt/wt) directly to the aqueous
158 suspension (Figure 1, Panel B).
159 The pH of cellulose nanocrystal suspensions, was raised to approximately 9 by using a 0.25 %wt
160 NaOH solution, aimed at assuring the thermal stability of cellulose nanocrystals aqueous
161 suspensions (Fortunati et al., 2012; Petersson, et al., 2007) and, finally, the aqueous solutions were
162 freeze dried to obtain cellulose powder.
163
164 **2.3 PLA_PBS blend preparation and characterizations**
165 PLA and PLA_PBS based films were prepared by means of solvent casting. Firstly, PLA (1 g) was
166 dissolved in 25 mL of chloroform ($CHCl_3$) with stirring at room temperature (RT). The obtained
167 solution was cast onto a *Petri* dish and then dried for 24 h at RT (Figure 1, Panel B). PLA and PBS
168 pellet were solvent blended at three different weight ratios adding 10, 20 or 30 wt % of PBS into
169 PLA solution (90/10, 80/20 and 70/30 PLA/PBS) namely PLA_10PBS, PLA_20PBS and
170 PLA_30PBS. The polymers were stirred at RT and exposed to sonication (Vibracell, 750W) for 10
171 minutes in an ice bath, after that solution was cast onto a *Petri* dish and then dried for 24 h at RT.
172 The microstructure of the PLA_PBS blend fractured surfaces was investigated by scanning electron
173 microscope, (FESEM, Supra 25-Zeiss), after gold sputtering of the surfaces to provide enhanced
174 conductivity and observed using an accelerating voltage of 2.5 kV.
175 The mechanical behaviour of PLA_PBS films was evaluated by tensile tests on the basis of UNI
176 ISO 527 standard, performed on rectangular probes (50 mm x 10 mm) with a crosshead speed of 1
177 mm min^{-1}, a load cell of 500 N and an initial gauge length of 25 mm. The elastic modulus (E), the

yield stress and strain (σ_y, ε_y) the tensile strength (σ_B) and elongation at break (ε_B) were calculated from the resulting stress-strain curves. The measurements were done at RT and at least five samples were tested.

Thermal characterization was done by both differential scanning calorimetric (DSC) and thermogravimetric analysis (TGA). DSC measurements were carried out on a TA Instruments DSC Q200 in modulated mode (TA Instruments Inc., USA) equipped with Universal Analysis 2000 software under nitrogen atmosphere in the range of -60 to 200 °C at 2 °C min^{-1}, applying two heating and one cooling scan. Melting and cold crystallization temperatures and enthalpies (T_m, T_{cc} and ΔH_m, ΔH_{cc}) and glass transition temperature (T_g) were determined from the first heating scan. The period and the amplitude of modulation were respectively 60 s and 2 °C. TGA (Seiko Exstar 6300) experiments from 30 to 600 °C at 10 °C min^{-1} under a nitrogen atmosphere were performed for each sample.

2.4 PLA_PBS bionanocomposite preparation

PLA or PLA_20PBS (the PBS content was selected on the base of previous described optimization procedure) based bionanocomposites, containing 1wt % and 3 wt% of unmodified (CNC) and surfactant modified (s-CNC) cellulose nanocrystals, were manufactured. After freeze-drying procedure, the organic solvent was added to CNC or s-CNC and exposed to sonication (Vibracell, 750W) for 1 min in an ice bath. Binary film based on PLA matrix was also produced for comparison. Neat PLA loaded with 1wt % and 3 wt% of unmodified CNC and surfactant modified s-CNC were processed: a specific amount of CNC or s-CNC suspension was added to the previously prepared PLA solution and then cast at RT.

Binary (PLA_CNC or PLA_s-CNC) and ternary (PLA_20PBS_CNC or PLA_20PBS_s-CNC) films with a thickness of approximately 50 μm were obtained.

2.5 Morphological, thermal and mechanical characterization of PLA and PLA_PBS based bionanocomposites

The microstructure of PLA and PLA_PBS based bionanocomposite surfaces and fractured surfaces was investigated by scanning electron microscope (FESEM, Supra 25-Zeiss), as previously described for PLA_PBS blend optimization. The surface properties of the produced bionanocomposites formulations were investigated by both atomic force microscopy (AFM) and optical microscopy. The AFM analysis was performed by a Nanoscope III.a Scanning Probe Microscope, (Multimode 8, Bruker AXS, Inc. Santa Barbara, California, USA), with a NanoScope® V controller electronics. Measurements were taken from several areas of the film surface (50 x 50 μm and 3 x 3 μm), using the phase imaging mode. Optical analysis was carried out by light microscopy using an optical microscopy (DM/LP Leica Microsystems, Wetziar GmbH) with a CCD camera incorporated, which allowed acquiring images from different samples. Images of films containing or not cellulose nanocrystals were acquired by using x 200 magnification.

The transparency of the films was determined from the surface reflectance spectra by using a spectrocolorimeter CM-3600d (Minolta Co, Tokyo, Japan) with a 30 mm illuminated sample area by applying the Kubelka–Munk theory for multiple scattering to the reflection spectra. This theory was based on that the light passes through the film, it is partially absorbed and scattered, which is quantified by the absorption (K) and the scattering (S) coefficients. Internal transmittance (T_i) of the films was quantified using equation 1. In this equation R_0 is the reflectance of the film on an ideal black background. Parameters a and b were calculated by equations 2 and 3, where R is the reflectance of the sample layer backed by a known reflectance R_g. The reflection spectra on the white and black background was determined from 400 to 700 nm. Measurements were taken in triplicate for each formulation.

$$T_i = \sqrt{(a - R_0)^2 - b^2} \qquad \text{(Eq. 1)}$$

227 $$a = \frac{1}{2}(R + \frac{R_0 - R + R_g}{R_0 R_g}) \qquad \text{(Eq. 2)}$$

228 $$b = (a^2 - 1) \qquad \text{(Eq. 3)}$$

229 Gloss was measured using a flat surface gloss meter (Multi-Gloss 268, Minolta, Langenhagen,
230 Germany) at an incidence angle of 60º, according to the ASTM standard D523 (ASTM, 1999).
231 Gloss measurements were performed over a black matte standard plate and were taken in triplicate.
232 Results were expressed as gloss units, relative to a highly polished surface of standard black glass
233 with a gloss value close to 100.
234 The mechanical (tensile test) and thermal (TGA and DSC) behaviour of PLA and PLA_PBS based
235 bionanocomposite films were evaluated as previously reported in the PLA_PBS blend optimization
236 paragraph.
237
238 **2.6 Barrier properties of PLA and PLA_PBS based bionanocomposites**
239 The barrier properties of PLA and PLA_PBS based formulations were evaluated by both water
240 vapour permeability (WVP) test and oxygen transmission rate measurements. WVP was evaluated
241 following the gravimetric method ASTM E96-95 (ASTM, 1995) by using Payne permeability cups
242 (Payne, elcometer SPRL, Hermelle/sd Argenteau, Belgium) of 3.5 cm diameter. Deionised water or
243 lithium chloride oversaturated solution were used inside the testing cups to achieve 11 or 100 % RH
244 respectively, on one side of the film, meanwhile an oversaturated magnesium nitrate solution was
245 used to control the RH (53 % RH) on the other side of the film. The relative humidity of the tests
246 was selected according to the final use of the flexible films as package material, thus simulating the
247 contact with fresh food, such as meat or fresh cut fruit or very low water activity products,
248 respectively. A fan placed on the top of the cup was used to reduce resistance to water vapour
249 transport. Water vapour transmission rate measurements (WVTR) were performed at 25 ºC. To
250 calculate WVTR, the slopes in the steady state period of the weight loss vs. time curves were

251 determined by linear regression. WVP was calculated according to Cano et al., 2014 (Cano,
252 Jiménez et al., 2014). For each type of film, WVP measurements were taken in quadruplicate.
253 The oxygen barrier capacity of PLA and PLA_PBS based bionanocomposite films was evaluated by
254 measuring oxygen permeability (OP) by means of an Ox-Tran 1/50 system (Mocon, Minneapolis,
255 USA) at 25 °C (ASTM Standard Method D3985-95, 2002). Measurements were taken at 53 % in
256 films previously equilibrated at the same RH. Films were exposed to pure nitrogen flow on one side
257 and pure oxygen flow on the other side. The OP was calculated by dividing the oxygen transmission
258 rate by the difference in the oxygen partial pressure on the two sides of the film, and multiplying by
259 the average film thickness. At least three replicates per formulation were taken into account.
260

261 **2.7 Overall migration of PLA and PLA_PBS based bionanocomposites**

262 The overall migration analysis of PLA and PLA_PBS bionanocomposites permits to simulate the
263 use of proposed package formulation with two different food simulants in order to investigate the
264 possible application of the produced PLA based bionanocomposites for fresh-food packaging. The
265 test was run in triplicate in simulant A (10% (v/v) ethanol water solution) and alternative simulant
266 to D2 (isooctane) according to current legislation Commission Regulation (EU) No 10/2011.
267 Rectangular strips of 10 cm^2 in 10 mL of food simulants were used. Samples were kept in the
268 ethanol solution in a controlled atmosphere at 40 °C for 10 days, while samples in isooctane were
269 kept at 20 °C for 2 days according to EN 1186-1:2002. At the end of the experiment, films were
270 removed and the simulants evaporated in agreement with the European Standard 1186-3:2002.
271 Materials and articles in contact with foodstuffs - Plastics - Part 3: Test methods for overall
272 migration into aqueous food simulants by total immersion. The residues were weighed with an
273 analytical balance with ± 0.01 mg precision and the migration value in mg kg^{-1} of the/each simulant
274 was determined.
275

2.8 Disintegrability in composting conditions of PLA and PLA_PBS based bionanocomposites

Disintegrability in composting conditions was carried out following the European standard ISO 20200. The test determines, at laboratory-scale, the degree of disintegration of plastic materials under simulated intensive aerobic composting condition. The degree of disintegration *D* was calculated in percent by normalizing the sample weight at different days of incubation to the initial weight by using Equation (4):

$$D = \frac{m_i - m_r}{m_i} * 100 \qquad \text{(Eq. 4)}$$

where:

m_i= is the initial dry plastic mass;

m_r= is the dry plastic material after the test.

PLA and PLA_PBS bionanocomposite films of dimension 15 mm x 15 mm x 0.03 mm were weighed and buried into the organic substrate at 4-6 cm depth in the perforated boxes guarantying the aerobic conditions and incubated at 58 ºC and 50 % of humidity. The systems can be considered disintegrable according to the European standard when 90% of the plastic sample weight shall be lost within 90 days of analysis. In order to simulate the disintegrability in compost, a solid synthetic waste was prepared, mixing sawdust, rabbit food, compost inoculum supplied by Genesu S.p.a., starch, sugar, oil and urea. The samples tested were taken out at different times (1, 3, 8, 10, 13, 15 and 17 days), washed with distilled water and dried in a oven at 37 °C for 24 h. The photographs on the samples were taken for visual comparison.

2.9 Compost study

The composting process was carried out as previously described, in order to evaluate the quality of compost obtained by the degradation of PLA and PLA_PBS bionanocomposite films (PLA_PBS compost) compared to the same mixture without the tested material used as control (CNT compost).

300 During the incubation period, samples of PLA_PBS and CNT composts were collected at 20 and 90
301 days, in order to evaluate the active phase of composting and the quality of the final compost,
302 respectively. The starting mixture used as control had a moisture content of 53.9%, a pH and
303 electrical conductivity (EC) value of 7.2 and 0.93 dS m^{-1}, respectively.
304 Moisture content was determined by weight loss upon drying at 105 °C in an oven for 24 h.
305 Electrical conductivity and pH were determined on the fresh samples in a 1:10 compost:water
306 extract ratio (ANPA, 2001). Total volatile solids (VS) were determined by weight loss upon ashing
307 at 550 °C for 24 h in a muffle furnace. Total VS were used to calculate the organic matter (OM)
308 loss during composting, according to the equation described by Viel et al. (1987) and recently used
309 also by Altieri et al. (2011) and Gigliotti et al. (2012) to describe OM loss during composting of
310 olive mill waste**.** Total organic carbon (TOC) was determined on dried samples by an elemental
311 analyser (EA 1110 Carlo Erba, Milan, Italy; ANPA, 2001), whereas fresh samples were used for
312 determination of total Kjeldahl-N (TKN) and NH^{+}_{4}-N (ANPA, 2001). Total organic N was
313 determined by the difference between TKN and NH^{+}_{4}-N.
314 Germination index (GI) was determined by means of a *Lepidium sativum* L. seed germination
315 bioassay, as proposed by Zucconi et al. (1985) and modified by Said-Pullicino et al. (2007). In order
316 to evaluate the quality of the final compost, total P, total K and total Cd, Cu, Hg, Ni, Pb and Zn
317 contents were determined by applying ANPA methods (2001).
318

319 **2.10 Statistical analysis**

320 Results were analysed by analysis of variance (ANOVA), using the Statgraphics Plus 5.1. Program
321 (Manugistics Corp., Rockville, MD). To differentiate samples, Fisher's least significant difference
322 (LSD) was used at the 95 % confidence level.

323 **Results and Discussion**

324 **3.1. Optimization of the PBS content in PLA_PBS blend**

Figure 2 shows the morphological, mechanical and thermal characterization of PLA_PBS blends with different content of PBS: 10, 20 and 30 %wt respect to PLA. The fractured surfaces (cross-sections) of PLA and PLA_PBS blends were investigated by FESEM (Figure 2,a) to evaluate the influence of different ratio of PBS in the PLA matrix. A relatively smooth fractured surface was observed for the PLA film, while PLA_PBS formulations exhibit a typical morphology of this polymeric combination, in fact, as it possible to observe a phase separation in PLA_PBS blends with a typical formation of nodules induced by the presence of PBS as previously observed in the literature (Bhatia et al., 2007; Persenaire et al., 2014). The dimension of nodules increases PBS content in PLA matrix, as well identified in PLA_30PBS film. Nevertheless, the PLA_20PBS formulation is characterized by smaller and better dispersed PBS nodules than PLA_10PBS and PLA_30PBS films. Figure 2,b shows the tensile strength and the elongation at break of PLA and PLA_PBS formulations. The incorporation of PBS causes the reduction in tensile strength, as already observed by Bhatia et al 2007 and Persenaire et al. 2014 and an increase in deformation at break up to PBS content lower than 20 wt %.The reduction of the elongation at break in PLA_30PBS film could be due to low miscibility of both polymer as observed by FESEM investigation. The inclusion of PBS particles affects the material resistance due to the presence of discontinuities, which weaks the cohesion of the matrix and reduce its mechanical performance. The thermal behaviour of PLA and PLA_PBS formulations was evaluated by DSC to study the effects of different ratio of PBS on the PLA thermal properties. The obtained curves are reported in Figure 2,c and the results are also summarized in Table 1. PLA films show only one melting peak while PLA_PBS films show two melting peaks (see Figure 2,b), indicating that each polymeric components crystallize individually and the polymeric blends are immiscible (Bhatia, Gupta, Bhattacharya & Choi, 2007). The first melting peaks around 111 °C is present only in PLA_PBS formulations and the enthalpy values increase with increasing content of PBS into PLA matrix. Moreover, the enthalpy associated with the second melting peak decrease with increasing contents

of PBS, with values ranging from 25 to 24, 23 and 20 (J g^{-1}) for PLA, PLA_10PBS, PLA_20PBS and PLA_30PBS, respectively. The cold crystallization of neat PLA is centred around 98°C and, in the case of PLA_PBS formulations, the cold crystallization is shifted to lower temperature as a consequence of blending. Nevertheless, the cold crystallization of PLA corresponds with the melting peaks of PBS and this phenomenon obstacle the visualization of cold crystallization peak of PLA into the PLA_PBS films.

The thermal behaviour of PLA and PLA_PBS based formulations was also investigated by thermogravimetric analysis, with the aim of evaluating the effect of different content of PBS on the degradation behaviour of PLA matrix and the results are reported in Table 1. PLA decomposes in single one step while PLA_PBS formulations decompose in two steps due to the presence of PBS in PLA matrix in a separated phase. The maximum degradation temperature is centred at 364 °C for PLA, while the two degradation temperatures of PLA_PBS were centred at around 364 and 394 °C. Finally, no so evident modifications of the degradation temperatures were observed adding different contents of PBS in PLA.

On the base of these results, PLA_20PBS appears as the best formulation suitable for the realization of PLA_PBS based ternary systems reinforced with CNC and s-CNC.

3.2. PLA_CNC and PLA_PBS_CNC bionanocomposite characterizations

3.2.1. Morphological investigation

The microstructure of the cross-section surfaces of PLA and PLA_20PBS based bionanocomposites was qualitatively analyzed by using FESEM (Figure 3), while the surface structure was analyzed by AFM, FESEM and optical microscope (Figure 4).

Fractured surfaces of PLA and PLA_20PBS, binary and ternary bionanocomposites, show an homogenous morphology and the absence of visible cellulose nanoreinforcements. Rougher fractured surfaces were observed for unmodified CNC based binary and ternary bionanocomposites

375 as a consequence of cellulose nanocrystals introduction, while smooth section surfaces were
376 observed for surfactant modified s-CNC based systems. Nevertheless, the PLA and PLA_20PBS
377 based systems reinforced with CNC and s-CNC show a compact structure respect to PLA and
378 PLA_20PBS based films suggesting that unmodified and modified cellulose nanocrystals increase
379 the interfacial adhesion of two polymeric phases as observed in literature (Arrieta et al., 2014). The
380 higher interaction of the two phases, due to the presence of CNC and s-CNC, positively influences
381 the barrier properties, determining a lower oxygen and water vapour permeability in comparison
382 with neat PLA and PLA_20PBS as described in the following sections.
383 AFM images show the topographic analysis of PLA and PLA_20PBS based bionanocomposites
384 obtained by using Phase Imaging mode derived from Tapping Mode. In PLA and PLA_20PBS
385 based bionanocomposites, heterogeneous response of different phase can be detected. In the ternary
386 systems the different phases can be related to the presence of PBS. AFM images underline a good
387 distribution of cellulose nanocrystals modified with the surfactant into the matrix and in
388 PLA_20PBS based films.
389 FESEM investigation of PLA and PLA_20PBS based systems shows smooth surface of PLA
390 bionanocomposites and a typical nodular structure of PLA_PBS based systems induced by the
391 presence of PBS (Lin, Chen, et al. 2015; Malwela, Sinha Ray, 2014). As it is possible to see at
392 higher magnification in PLA_20PBS_3s-CNC formulations, the s-CNC are well dispersed also on
393 the surface of nodules (see insert).
394 Optical microscope images of the bionanocomposite film surfaces show a clear presence of
395 heterogeneous materials due to the agglomeration of CNC created during the processing or cast
396 phase identifiable as brown areas. The aggregation phenomena is more evident for PLA_3CNC and
397 PLA_20PBS_3CNC. On the other hand, the surfaces of s-CNC based systems are more
398 homogeneous, and this morphology highlights that the surfactant modified cellulose nanocrystal are
399 well dispersed into PLA and PLA_20PBS based systems.

400

401

402 *3.2.2. Thermal properties*

403 Differential scanning calorimetry was used to investigate the effect of cellulose nanocrystals and
404 PBS on glass transition, crystallization and melting phenomena of PLA and PLA_20PBS
405 bionanocomposites. The thermal properties obtained for the first heating scan are summarized in
406 Table 1. No significant changes were observed in the glass transition temperature (T_g) between neat
407 PLA and PLA binary films reinforced with both content of s-CNC while a slight shift to higher
408 temperatures was observed in the case of PLA_3CNC and in PLA_20PBS based
409 bionanocomposites. Moreover, the addition of s-CNC in binary and ternary films shifts the cold
410 crystallization phenomenon to lower temperature indicating that the presence of cellulosic
411 nanoreinforcements favours the crystallization, underlining the combined effect of s-CNC and PBS
412 as nucleating agents (Fortunati et al., 2012). On the contrary, the addition of unmodified cellulose
413 nanocrystals shifts to higher temperature or does not modify the T_{cc} underlining also the effect of
414 surfactant based modification. PLA films show only one melting peak while PLA_20PBS based
415 films show two melting peaks (see Figure 2,b), indicating that each polymeric components
416 crystallize individually and the polymeric blends are immiscible (Bhatia et al., 2007). The double
417 melting behaviour observed in the peak relative to PLA melting with one peak at around 147 °C and
418 the second one at 153 °C, can be attributed to the formation of different typologies of crystals. In
419 particular, the double peak of melting is due to the formation of small and imperfect crystals during
420 the cooling that modify through melting and recrystallization at low heating rates (Arrieta et al.,
421 2014; Fortunati et al., 2015). The melting enthalpy values related to PLA component increases
422 adding the content of cellulose nanocrystals; this behaviour highlights how high quantities of
423 crystals melt. No evident variation on the melting enthalpy values is observed for the PBS
424 component.

425 The thermal behaviour of PLA and PLA_20PBS based bionanocomposites was also evaluated by
426 thermogravimetric analysis and the effect of introduction of CNC and s-CNC were summarized in
427 Table 1. The evaluation of thermogravimetric degradation of bionanocomposites is consider as an
428 important property, taking into account the practical application at industrial level where the
429 polymer or the polymeric blends can be used and processed. As previously reported, PLA matrix
430 decomposes in a single step centred around 364 °C, while PLA_20PBS decomposes in two steps
431 the first one can be ascribed to the presence of PLA and the second one is due to PBS presence. No
432 significant influence of the unmodified cellulosic nanofiller on the degradation temperature of the
433 PLA and PLA_20PBS based formulations was observed (Fortunati et al., 2014). Moreover,
434 different behaviour was observed using surfactant modified cellulose nanocrystals. In this case, the
435 maximum degradation temperature shifted of about 13-18 °C to lower temperature for PLA_1s-
436 CNC and PLA_3s-CNC in accord to other previous research (Fortunati et al., 2015); this reduced
437 thermal stability can be easily attributed to the lower thermal stability of the CNC detected around
438 327 °C as described in a previous research of Luzi et al. 2014 Nevertheless, in PLA_20PBS based
439 formulations only the peak relative to the maximum degradation temperature of PLA shifted of
440 about 20 °C to lower temperatures.
441
442 *3.2.3. Mechanical behaviour*
443 The mechanical behaviour of PLA and PLA_20PBS based bionanocomposites was evaluated by
444 means of tensile tests and the results are summarized in Table 2. As previously reported (Fortunati
445 et al., 2014), the addition of unmodified CNC produces an increase in Young's modulus and
446 strength at break values in binary and ternary systems, highlighting the reinforcement effect induced
447 by CNC. This effect is more evident in the case of the 3 wt% based formulations that showed the
448 highest Young's modulus (1540 MPa and 1130 MPa obtained for PLA_3CNC and
449 PLA_20PBS_3CNC, respectively). Moreover, a decrease in the elongation at break of the CNC

450 based bionanocomposites with respect to the PLA matrix was observed, with a more pronounced
451 effect for the PLA_3CNC system, confirming the increase in brittleness induced by the addition of
452 unmodified CNC.
453 The surfactant modified s-CNC based formulations presented a different behaviour. The increase in
454 elongation at break values obtained for all PLA based formulations is relevant, showing an evident
455 ductile behaviour of the materials. The data obtained through tensile testing validated the
456 plasticization effect induced by the s-CNC discussed in the thermal and morphological sections,
457 suggesting the possibility of modulating the mechanical properties according to application
458 requests, introducing unmodified CNC or surfactant modified s-CNC to the biodegradable polymer
459 matrix.
460
461 *3.2.4. Barrier and optical properties*
462 The evaluation of barrier properties is one of the most important requirement for food packaging.
463 The results of this assessment are summarized in Table 3. The control of atmosphere and the
464 moisture of food contained into the packaging permits to maintain its safety and its quality without
465 compromising the organoleptic quality. The goal of food packaging is not only to contain and
466 preserve food during the transport and storage, but also the reduction of external contaminations,
467 thus increasing its shelf-life (Rhim et al., 2013).
468 Reduction of 21 % and 25 % in OP was detected for PLA_3 CNC and PLA_3s-CNC, respectively.
469 The use of cellulose nanocrystals increase the tortuosity of gas molecules path way through the
470 polymer structure (Fortunati, et al., 2013) Moreover, this behaviour underlines that cellulose
471 nanocrystals modified with the commercial surfactant are well dispersed on the surface of PLA
472 matrix (see AFM investigation Figure 4) and this configuration result the best compromise for
473 modulation and control of gases permeability. According to Bathia et al. 2010 the addition of PBS
474 influences positively the OP result (ca. 32 %). A significant difference ($p<0.05$) of OP values was

obtained for PLA and PLA_20PBS based bionanocomposites, underlining that the combined addition of cellulose nanocrystals and PBS into PLA is able to positively modify and reduce the oxygen permeability. Finally, PLA_20PBS_3s-CNC is absolutely the best formulation (OP reduction of 47 %) that combined the double effect, due to the presence of surfactant modified cellulose nanocrystals and PBS addition.

The water vapour permeability was evaluated at 25 °C and at two different conditions of relative humidity; the first one at 11-53% RH and the second one at 100-53 %RH and the results are summarized in Table 3. The data obtained are in accord to other previous research (Sanchez-Garcia, Lagaron, 2010). The WVP of bionanocomposite films changed significantly ($p < 0.05$) comparing the values obtained for all formulations by WVP tested at 25°C and at 11-53% RH and at 100-53 RH. PLA formulation loaded with 3 wt % of CNC and s-CNC show poor barrier properties in the case of the test performed at 100-53 % of RH and at 25 °C, which could be due to the hydrophilic nature of CNC and of commercial surfactant. The reduction values obtained for WVP at 11-53% RH are higher respect to values obtained for WVP at 100-53% RH. The relatively high humidity conditions could reduce and compromise the water vapour barrier properties of PLA and PLA_20PBS based formulations. The highest reduction of WVP values, 44% and 30 % in the case of the test conducted at 11-53% and 100-53 % of RH, respectively was observed for PLA_20PBS_1s-CNC.

Table 3 shows also the values of internal transmittance (T_i) at 450 nm and the gloss values at 60° of PLA and PLA_20PBS bionanocomposites. The gloss and transparency of the films are relevant properties for food packaging applications since determine the appearance of the coating. According to Kubelka-Munk theory, high values of T_i are associated to translucency level and structural homogeneity and their high degree of transparency, while low T_i values are related to a high opacity and structural heterogeneity. In fact, the presence of more heterogeneous structures promotes light dispersion and a reduction of internal transmittance. The highest T_i value was found

for neat PLA and no significant changes ($p<0.05$) were detected for all the produced PLA based bionanocomposites.

The gloss of bionanocomposites was greatly affected by the presence of both PBS and nanoreinforcements. In the case of the binary bionanocomposites reinforced with CNC the values of gloss decrease as a function of the filler percentage, and this result can be related to the presence of agglomerates on the surface as observed by optical microscopy investigation. Different behaviour was observed in the binary bionanocomposites reinforced with s-CNC; being the values of the gloss increased respect to PLA film (Table 3).This effect can be related to the good distribution of modified cellulose nanocrystals on the surface of binary systems as observed to AFM investigation. Moreover, the increase of gloss should be also attributed by the optical and chiral properties of CNC (Bondeson et al., 2013). In the case of PLA_20PBS bionanocomposites reinforced with CNC, the values of gloss decreases as function of the filler percentage,, which can be related to the presence of agglomerates on the surface, as observed by optical microscopy. On the other hand, the gloss increases in the ternary systems reinforced with s-CNC respect to PLA_20PBS bionanocomposites reinforced with the unmodified cellulose nanocrystals; and this effect can be due to the best distribution of surfactant modified cellulose nanocrystals into PLA_20PBS based systems.

3.2.5 Overall migration

Overall migration tests with food simulants were carried out and the results are shown in Figure 5. The test permits to simulate and demonstrate, by using two different simulants (A and substitutive D2), the behaviour of potential food packaging in contact with the foodstuff. The overall migration levels for all the studied formulations are lower than the migration limits for food contact materials, 60 mg kg^{-1} of simulant, established by the current European legislation, demonstrating the possible practical application of the produced films in the food packaging field.

525 Specifically, after 10 days of incubation at 40 °C in ethanol 10% (v/v), PLA neat film migration
526 level is around 0.087 mg kg^{-1} while the maximum migration level is detected for PLA_20PBS_3s-
527 CNC formulation (0.191 mg kg^{-1}). Analyzing the obtained results by using isooctane, there was an
528 evident effect of both cellulose nanocrystal type and amounts and PBS presence that increased
529 migration values. The maximum value of 0.137 mg kg^{-1}, was detected also in this case of
530 PLA_20PBS_3s-CNC.
531 The increase in the migration levels for both the studied simulants is due to induced structure
532 observed in the case of s-CNC containing systems, that resulted well dispersed and preferentially
533 disposed on the surfaces of PLA_s-CNC and PLA_PBS_s-CNC systems (due to the effect of the
534 applied modification) as proved by AFM investigations (Heux et al., 2000).
535
536 *3.2.6. Disintegrability in composting conditions*
537 The disintegrability in composting conditions of PLA and PLA_20PBS based bionanocomposites
538 represents an interesting and attractive property for packaging applications that simulates the post-
539 use of plastics (Kale et al., 2007). The test permits to evaluate if the produced packaging can be
540 disintegrate completely in contact with composting soil by microorganisms, including fungi and
541 bacteria without affecting the environmental pollution. The disintegration starts when the molecular
542 weight of PLA reaches about 10.000-20.000 g mol^{-1}. The microorganisms metabolize the
543 macromolecules of PLA and PLA_20 PBS based films as organic matter, converting them to water,
544 humus and carbon dioxide (Kale et al., 2007). The use of cellulosic nanoreinforcements influence
545 the biodegradation in compost of PLA and PLA_20PBS as a consequence of their hydrophilicity
546 nature (Fukushima et al., 2009; Luzi et al., 2015). On the contrary, the presence of PBS into PLA
547 matrix obstacle the disintegrabibility as a consequence of higher crystalline nature induced by PBS
548 addition.

549 Figure 6 shows the visual observation (Figure 6,a), the disintegrability values (Figure 6,b) of the
550 PLA and PLA_20PBS based formulations reinforced with CNC and s-CNC taken out at different
551 times of composting while the composting soil appearance at different time of incubations is shown
552 in Figure 6,c.
553 Figure 6,a shows the visual characteristics of different formulations at different time of incubations
554 evidencing that after only three days of incubation, the samples start to change their appearance,
555 becoming white and deformed. The whitening process and the opacity are attributed to change in
556 the refractive index due to water absorption, that induces an increase of the crystallinity during
557 degradation (Bitinis et al., 2013). Figure 6,b shows that all the materials reach a degree of
558 disintegration exceeding 90% after 17 days of composting, in particular PLA_s-CNC based
559 formulations disintegrate completely after 13 days under compost soil, while neat PLA and
560 PLA_CNC and PLA_20PBS based bionanocomposites films disintegrate after 15 and 17 days,
561 respectively. Moreover, after 8 days of incubation, all the studied formulations become breakable
562 and the weight loss considerably increases; the PLA_CNC based formulations show a reduction in
563 weight of 30-40%, while the PLA_20PBS based systems show a lower reduction, reaching a 20-30
564 % of disintegrability. The lower disintegrability of PLA_20PBS bionanocomposites is related to
565 high crystallinity induced by the presence of PBS (Kim et al., 2005) as commented before. The
566 higher values of disintegration are observed for the formulations reinforced with s-CNC. This
567 different behaviour is correlated to the different morphology of cross sections and to the presence of
568 hydrophilic surfactant used to improve the dispersion of cellulosic nanofillers in PLA that resulted
569 well dispersed on the surface of PLA_20PBS based bionanocomposites. Finally, Figure 6,c shows
570 the images of composting soil at different time of incubations underling how the maturity of soil
571 influence the visual aspect. The colour of soil change immediately after only one day of test
572 becoming brown and reaches its maturation after 2 weeks.
573

574 *3.2.7 Organic matter degradation and compost quality*

575 During the composting process, it was possible to observe a loss of OM in both composts used in
576 the experiment (Table 4). It was interesting to notice that the OM loss was more evident in the
577 PLA_PBS compost after 90 days of incubation, whereas in the CNT compost occurred just in the
578 first 20 days of process. The slower mineralization of the OM in the PLA_PBS samples might be
579 related to the presence of these materials, subjected to a chemical degradation of polymer as a result
580 of hydrolysable functional groups in the polymer backbone (Kale et al., 2007). The C/N ratio did
581 not change during the composting process in the CNT compost, whereas an increase was observed
582 after 90 days of incubation in PLA_PBS samples, probably due to a loss of N in the second part of
583 the process (data not shown). Both composts reached a C/N < 25 according to the limit values for
584 an adequate agronomical use of compost. The C/N represent a good indicator of N availability for
585 the process, in fact it is well known that C/N decrease is an indicator of stability for composting
586 processes (Gigliotti et al., 2012). Germination index was evaluated during the composting process
587 in order to verify the presence or the new formation of phytotoxic compounds during composting.
588 Results of GI are reported in Table 4 and they show that during the stabilisation process is
589 noticeable the improving of this parameter, which increases at the end of composting, leading to
590 values > 60% in both tested compost. This suggest that the phytotoxicity decrease during the
591 composting and the addition of the PLA_PBS based bionanocomposites did not affect the
592 development of the whole process, even if a low germination index occurred after 20 days of
593 aerobic treatment. These findings might be explain with the release of toxic compounds during the
594 first stages of the composting, such as ammonia, alcohols and mineral salts (Said-Pullicino et al.,
595 2007). The chemical composition of the obtained composts was reported in Table 5. The moisture
596 content in both composts were still high (>50%) after 90 days of composting, but this might be
597 explained by the test protocol used that provided water addition during the laboratory scale
598 experiment. Results of the heavy metals showed a low concentration in both composts; these

findings were expected, since the starting mixture was composed by materials poor in contaminant elements. Total P and total K content did not show high values as generally found in the compost used as fertiliser. Moreover is interesting to note that the DH, widely used as indicator of the formation of humic-like stable compounds (Ciavatta et al., 1988; Mondini et al., 1996; Alburquerque et al., 2009), showed a value > 50% in both tested composts after 90 days of process.

4. Conclusions

Poly(lactic acid) (PLA) and poly(lactic acid) (PLA)/ poly(butilene succinate) (PBS) based bionanocomposite films reinforced with unmodified cellulose nanocrystals (CNC) and surfactant modified cellulose (s-CNC) extracted from *Carmagnola* carded hemp fibres, were successfully produced by a solvent casting method.

Morphological, mechanical and thermal characterizations were performed to select the best content of PBS in PLA matrix and the results suggested that 20 wt % of PBS guarantees a valid compromise to maintain and modulate the mechanical properties and thermal properties of PLA and also its topography.

Concerning the PLA_PBS bionanocomposites, the results of thermal characterization underlined the ability of both PBS and cellulose nanocrystals to act as nucleating agents, with an evident improvement in PLA oxygen and water vapour permeability.

All the produced binary systems maintained the optical transparency of the PLA matrix, while the addition of PBS reduced the transparency and the gloss, as consequence of high crystallinity induced by the polymer. The presence of the surfactant on the nanocrystal surface favoured their dispersion in the polymer matrix. Data from mechanical tests confirmed the plasticization effect induced by s-CNC, suggesting the possibility of modulating mechanical properties according to application requests. The tensile strength and modulus decreased with PBS content. Finally, the

migration levels for all the studied bionanocomposites, tested with two food simulants, were maintained below the European legislative limits.

The disintegrablity under composting conditions revealed that the presence of surfactant facilitate the disintegration, while, the presence of PBS reduce the disintegration values. In any case, all the bionanocomposites disintegrate in less than 17 days. The study of the composting process and of the relative chemical parameters, confirmed that mostly the OM loss occurs in the active phase of composting (20 days), during which the degradation and the hydrolysis of the polymers took place. In addition, the monitoring of the curing phase (90 days) demonstrate that the obtained PLA_PBS compost did not contain phytotoxic molecules by an agronomical point of view. The present research suggests the possibility to produce high performance, sustainable and low-cost bionanocomposite formulations with tuneable properties for biodegradable food packaging applications.

Acknowledgements

Authors acknowledge Gesenu S.p.a. for compost supply.

References

Alburquerque, J.A., Gonzálvez, J., Tortosa, G., Baddi, G.A., Cegarra, J., 2009. Evaluation of ‘‘alperujo’’ composting based on organicmatter degradation, humification and compost quality. Biodegradation, 20, 257-270.

Altieri, R., Esposito, A., Nair, T., 2011. Novel static composting method for bioremediation of olive mill waste. Inter Biodeter Biodegr 65, 786-789.

ANPA (Agenzia nazionale per la protezione dell’Ambiente) 2001. Metodi di analisi del compost. Manuali e linee guida 3, 2001.

Arrieta, M. P., López, J., Ferrándiz, S., Peltzer, M. A., 2013. Characterization of PLA-limonene blends for food packaging applications. Polym. Test. 32(4), 760-768.

Arrieta, M. P., Fortunati, E., Dominici, F., Rayon, E., Lopez, J., Kenny, J. M., 2014. Multifunctional PLA-PHB/cellulose nanocrystal films: Processing, structural and thermal properties. Carbohyd. Polym. 107, 16-24.

Arrieta, M. P., López, J., Hernández, A., Rayón, E., 2014. Ternary PLA–PHB–Limonene blends intended for biodegradable food packaging applications. Eur. Polym. J. 50(0), 255-270.

Auras, R., Harte, B., Selke, S., 2004. An overview of polylactides as packaging materials. Macromol. Biosci., 4, 835-864.

Bhatia, A., Gupta, R., Bhattacharya, S., Choi, H., 2007. Compatibility of biodegradable poly (lactic acid)(PLA) and poly (butylene succinate)(PBS) blends for packaging application. Korea-Australia Rheology Journal, 19(3), 125-131.

Bhatia, A., Gupta, R. K., Bhattacharya, S. N., Choi, H. J., 2010. Effect of clay on thermal, mechanical and gas barrier properties of biodegradable poly (lactic acid)/poly (butylene succinate)(PLA/PBS) nanocomposites. Int. Polym. Process. 25(1), 5-14.

Bhatia, A., Gupta, R. K., Bhattacharya, S. N., Choi, H. J., 2012. Analysis of gas permeability characteristics of poly (lactic acid)/poly (butylene succinate) nanocomposites. J. Nanomat. 2012, 6.

Bitinis, N., Fortunati, E., Verdejo, R., Bras, J., Maria Kenny, J., Torre, L., Angel Lopez-Manchado, M., 2013. Poly(lactic acid)/natural rubber/cellulose nanocrystal bionanocomposites. Part II: Properties evaluation. Carbohyd. Polym. 96(2), 621-627.

Bondeson, D., Mathew, A., Oksman, K., 2006. Optimization of the isolation of nanocrystals from microcrystalline cellulose by acid hydrolysis. Cellulose 13(2), 171-180.

Cano, A., Jiménez, A., Cháfer, M., Gónzalez, C., Chiralt, A. 2014. Effect of amylose: amylopectin ratio and rice bran addition on starch films properties. Carbohyd. Polym. 111, 543-555.

671 Chaiwutthinan, P., Pimpan, V., Chuayjuljit, S., Leejarkpai, T., 2015. Biodegradable Plastics
672 Prepared from Poly (lactic acid), Poly (butylene succinate) and Microcrystalline Cellulose Extracted
673 from Waste-Cotton Fabric with a Chain Extender. J. Polym. Environ. 23(1), 114-125.
674 Chen, R., Zou, W., Wu, C., Jia, S., Huang, Z., Zhang, G., Yang, Z., Qu, J., 2014. Poly (lactic
675 acid)/poly (butylene succinate)/calcium sulfate whiskers biodegradable blends prepared by vane
676 extruder: Analysis of mechanical properties, morphology, and crystallization behavior. Polym.
677 Test., 34, 1-9.
678 Ciavatta, C., Vittori Antisari, L., Sequi P., 1988. A first approach to the characterization of the
679 presence of humified materials in organic fertilizers. Agrochimica 32, 510-517.
680 Cranston, E. D., Gray, D. G. 2006. Morphological and Optical Characterization of Polyelectrolyte
681 Multilayers Incorporating Nanocrystalline Cellulose. Biomacromolecules 7(9), 2522-2530.
682 Duncan, T. V. 2011. Applications of nanotechnology in food packaging and food safety: barrier
683 materials, antimicrobials and sensors. J Colloid Interf Sci, 363(1), 1-24.
684 El-Wakil, N. A., Hassan, E. A., Abou-Zeid, R. E., Dufresne, A. 2015. Development of wheat
685 gluten/nanocellulose/titanium dioxide nanocomposites for active food packaging. Carbohyd. Polym.
686 124, 337-346.
687 Fernandes, E. M., Pires, R. A., Mano, J. F., Reis, R. L., 2013. Bionanocomposites from
688 lignocellulosic resources: Properties, applications and future trends for their use in the biomedical
689 field. Prog Polym Sci, 38(10), 1415-1441.
690 Fortunati, E., Armentano, I., Zhou, Q., Iannoni, A., Saino, E., Visai, L., Berglund, L. A., Kenny, J.
691 M., 2012. Multifunctional bionanocomposite films of poly(lactic acid), cellulose nanocrystals and
692 silver nanoparticles. Carbohyd. Polym. 87(2), 1596-1605.
693 Fortunati, E., Peltzer, M., Armentano, I., Jimenez, A., Kenny, J. M., 2013. Combined effects of
694 cellulose nanocrystals and silver nanoparticles on the barrier and migration properties of PLA nano-
695 biocomposites. J Food Eng, 118(1), 117-124.

696 Fortunati, E., Puglia, D., Luzi, F., Santulli, C., Kenny, J. M., Torre, L., 2013. Binary PVA bio-
697 nanocomposites containing cellulose nanocrystals extracted from different natural sources: Part I.
698 Carbohyd. Polym. 97(2), 825-836.
699 Fortunati, E., Puglia, D., Monti, M., Peponi, L., Santulli, C., Kenny, J. M., Torre, L., 2013.
700 Extraction of Cellulose Nanocrystals from Phormium tenax Fibres. J. Polym. Environ. 21(2), 319-
701 328.
702 Fortunati, E., Luzi, F., Puglia, D., Dominici, F., Santulli, C., Kenny, J. M., Torre, L. 2014.
703 Investigation of thermo-mechanical, chemical and degradative properties of PLA-limonene films
704 reinforced with cellulose nanocrystals extracted from Phormium tenax leaves. Euro. Polym. J.
705 56(0), 77-91.
706 Fortunati, E., Luzi, F., Puglia, D., Petrucci, R., Kenny, J. M., Torre, L., 2015. Processing of PLA
707 nanocomposites with cellulose nanocrystals extracted from Posidonia oceanica waste: Innovative
708 reuse of coastal plant. Ind Crop Prod, 67, 439-447.
709 Fukushima, K., Abbate, C., Tabuani, D., Gennari, M., Camino, G., 2009. Biodegradation of poly
710 (lactic acid) and its nanocomposites. Polym. Degrad. Stabil. 94(10), 1646-1655.
711 Gandolfi, S., Ottolina, G., Riva, S., Fantoni, G. P., Patel, I., 2013. Complete chemical analysis of
712 carmagnola hemp hurds and structural features of its components. BioResources 8(2), 2641-2656.
713 Gigliotti, G., Proietti, P., Said-Pullicino, D., Nasini, L., Pezzolla, D., Rosati, L., Porceddu, P.R.
714 2012. Co-composting of olive husks with high moisture contents: Organic matter dynamics and
715 compost quality. Int. Biodeterior. Biodegrad. 67, 8-14.
716 Herrera, N., Mathew, A. P., Oksman, K., 2015. Plasticized polylactic acid/cellulose nanocomposites
717 prepared using melt-extrusion and liquid feeding: mechanical, thermal and optical properties.
718 Compos Sci Technol, 106, 149-155.
719 Heux, L., Chauve, G., Bonini, C. 2000. Nonflocculating and chiral-nematic self-ordering of
720 cellulose microcrystals suspensions in nonpolar solvents. Langmuir 16(21), 8210-8212.

721 Hsieh, Y.-L., 2013. Cellulose nanocrystals and self-assembled nanostructures from cotton, rice
722 straw and grape skin: a source perspective. J Mater Sci, 48(22), 7837-7846.
723 Hwang, S. Y., Yoo, E. S., Im, S. S., 2012. The synthesis of copolymers, blends and composites
724 based on poly (butylene succinate). Polym. J. 44(12), 1179-1190.
725 Itävaara, M., Karjomaa, S., Selin, J.-F., 2002. Biodegradation of polylactide in aerobic and
726 anaerobic thermophilic conditions. Chemosphere 46, 879-885.
727 Kale, G., Auras, R., Singh, S.P., 2007. Comparison of the degradability of poly (lactide) packages
728 in composting and ambient exposure conditions. Packag. Technol. Sci. 20, 49-70.
729 Kale, G., Kijchavengkul, T., Auras, R., Rubino, M., Selke, S. E., Singh, S. P. 2007. Compostability
730 of bioplastic packaging materials: an overview. Macromolecular bioscience, 7(3), 255-277.
731 Karamanlioglu. M., Houlden,A., Robson G.D., 2014. Isolation and characterisation of fungal
732 communities associated with degradation and growth on the surface of poly(lactic) acid (PLA) in
733 soil and compost. Inter Biodeter Biodeg 95, 301-310.
734 Khan, A., Khan, R. A., Salmieri, S., Le Tien, C., Riedl, B., Bouchard, J., Chauve, G., Tan, V.,
735 Kamal, M. R., Lacroix, M. 2012. Mechanical and barrier properties of nanocrystalline cellulose
736 reinforced chitosan based nanocomposite films. Carbohyd. Polym. 90(4), 1601-1608.
737 Kim, H. S., Yang, H. S., Kim, H. J. 2005. Biodegradability and mechanical properties of agro-
738 flour–filled polybutylene succinate biocomposites. J. Appl. Polym. Sci. 97(4), 1513-1521.
739 Lin, N., Dufresne, A., 2014. Nanocellulose in biomedicine: Current status and future prospect.
740 Euro. Polym. J. 59, 302-325.
741 Lin, N., Chen, Y., Hu, F., Huang, J., 2015. Mechanical reinforcement of cellulose nanocrystals on
742 biodegradable microcellular foams with melt-compounding process. Cellulose 22(4), 2629-2639.
743 Luzi, F., Fortunati, E., Puglia, D., Lavorgna, M., Santulli, C., Kenny, J. M., Torre, L., 2014.
744 Optimized extraction of cellulose nanocrystals from pristine and carded hemp fibres. Ind Crop Prod,
745 56(0), 175-186.

746 Luzi, F., Fortunati, E., Puglia, D., Petrucci, R., Kenny, J. M., Torre, L., 2015. Study of
747 disintegrability in compost and enzymatic degradation of PLA and PLA nanocomposites reinforced
748 with cellulose nanocrystals extracted from Posidonia Oceanica. Polym Degrad Stabil, 121, 105-115.
749 Malwela, T., Sinha Ray, S. 2014. Investigating the crystal growth behavior of biodegradable
750 polymer blend thin films using in situ atomic force microscopy. Macromol Mater Eng, 299(6), 689-
751 697.
752 Matos Ruiz, M., Cavaillé, J. Y., Dufresne, A., Gérard, J. F., Graillat, C., 2000. Processing and
753 characterization of new thermoset nanocomposites based on cellulose whiskers. Compos Interface,
754 7(2), 117-131.
755 Mondini, C., Chiumenti, R., da Borso, F., Leita, L., De Nobili, M., 1996. Changes during
756 processing in the organic matter of composted and air-dried poultry manure. Bioresource Technol,
757 55, 243-249.
758 Neto, W. P. F., Silvério, H. A., Dantas, N. O., Pasquini, D., 2013. Extraction and characterization of
759 cellulose nanocrystals from agro-industrial residue–Soy hulls. Ind Crop Prod, 42, 480-488.
760 Peelman, N., Ragaert, P., De Meulenaer, B., Adons, D., Peeters, R., Cardon, L., Van Impe, F.,
761 Devlieghere, F., 2013. Application of bioplastics for food packaging. Trends Food Sci Tech, 32(2),
762 128-141.
763 Persenaire, O., Quintana, R., Lemmouchi, Y., Sampson, J., Martin, S., Bonnaud, L., Dubois, P.,
764 2014. Reactive compatibilization of poly (l- lactide)/poly (butylene succinate) blends through
765 polyester maleation: from materials to properties. Polym Int, 63(9), 1724-1731.
766 Petersson, L., Kvien, I., Oksman, K., 2007. Structure and thermal properties of poly (lactic
767 acid)/cellulose whiskers nanocomposite materials. Compos Sci Technol, 67(11), 2535-2544.
768 Petrussi, F., De Nobili, M., Viotto, M., Sequi, P., 1988. Characterization of organic matter from
769 animal manures after digestion by earthworms. Plant Soil 105, 41-46.

770 Rhim, J.-W., Park, H.-M., Ha, C.-S. 2013. Bio-nanocomposites for food packaging applications.
771 Prog Polym Sci, 38(10), 1629-1652.
772 Saadi, Z., Rasmont, A., Cesar, G., Bewa, H., Benguigui, L., 2012. Fungal degradation of poly(l-
773 lactide) in soil and in compost. J. Polym. Environ. 20, 273-282.
774 Saïd Azizi Samir, M. A., Alloin, F., Paillet, M., Dufresne, A., 2004. Tangling effect in fibrillated
775 cellulose reinforced nanocomposites. Macromolecules, 37(11), 4313-4316.
776 Said-Pullicino, D., Erriquens, F.G., Gigliotti, G., 2007. Changes in the chemical characteristics
777 ofwater extractable organicmatterduring compostingand their influence on compost stability and
778 maturity. Bioresource Technol 98, 1822-1831.
779 Sanchez-Garcia, M. D., Lagaron, J. M., 2010. On the use of plant cellulose nanowhiskers to
780 enhance the barrier properties of polylactic acid. Cellulose, 17(5), 987-1004.
781 Sangwan, P., Wu, D.-Y., 2008. New insights into polylactide biodegradation from molecular
782 ecological techniques. Macromol. Biosci. 8, 304-315.
783 Silvério, H. A., Neto, W. P. F., Dantas, N. O., Pasquini, D., 2013. Extraction and characterization of
784 cellulose nanocrystals from corncob for application as reinforcing agent in nanocomposites. Ind
785 Crop Prod, 44, 427-436.
786 Stloukal, P., Kalendová, A., Mattausch, H., Laske, S., Holzer, C., Koutny, M. 2015. The influence
787 of a hydrolysis-inhibiting additive on the degradation and biodegradation of PLA and its
788 nanocomposites. Polym. Test. 41, 124-132.
789 Šturcová, A., Davies, G. R., Eichhorn, S. J., 2005. Elastic Modulus and Stress-Transfer Properties
790 of Tunicate Cellulose Whiskers. Biomacromolecules, 6(2), 1055-1061.
791 Torres, A., Li, S.M., Roussos, S., Vert M., 1996. Screening of Microorganisms for Biodegradation
792 of Poly (Lactic Acid) and Lactic Acid-Containing Polymers. Appl. Environ. Microbiol., 62, 2393-
793 2397.

Viel, M., Sayag, D., Peyre, A., André, L., 1987. Optimization of in-vessel co-composting through heat recovery. Biol Waste 20, 167-185.

Zucconi, F., Monaco, A., Forte, M., de Bertoldi, M., 1985. Phytotoxins during the stabilization of organic matter. In: Gasser, J.K.R. (Ed.), Composting of Agricultural and OtherWastes. Elsevier Applied Science Publishers, Barking, Essex, UK, pp. 73-85.

Commission Regulation EU 10/2011 - Commission Regulation (EU) No 10/2011 of 14 January 2011 on plastic materials and articles intended to come into contact with food.

European Standard EN 1186-1: 2002- Materials and articles in contact with foodstuffs. Plastics. Guide to the selection of conditions and test methods for overall migration.

UN EN ISO 20200 Determination of the degree of disintegration of plastic materials under simulated composting condition in a laboratory-scale test; 2006.

Figure and table captions

Figure 1: Panel A: Scheme of CNC extraction process from carded hemp fibres. Panel B: cellulose nanocrystals modification and PLA_PBS bionanocomposites production.

Figure 2: Morphological, mechanical and thermal properties of PLA and PLA_PBS based formulations. Different superscripts within the same colour column indicate significant differences among formulations ($p<0.05$).

Figure 3: Morphological investigation of PLA and PLA_20PBS bionanocomposites fracture surface.

Figure 4: AFM, FESEM, and Optical investigation of PLA and PLA_20PBS bionanocomposites surface.

Figure 5: Overall migration in 10% (v/v) ethanol and isooctane for PLA and PLA_20PBS bionanocomposites. Different superscripts within the same colour column indicate significant differences among formulations ($p<0.05$).

819 **Figure 6:**Visual observation(a), disintegrability values (b) and soil images (c) at different times.

820

821 **Table 1:** Thermal properties of PLA and PLA_20PBS based bionanocomposites.

822 **Table 2:** Mechanical properties of PLA and PLA_20PBS based systems.

823 **Table 3:** Barrier properties, internal transmittance (T_i) at 450 nm and gloss values at 60º for PLA

824 and PLA_20PBS based bionanocomposite formulations.

825 **Table 4:** Organic matter loss, C/N ratio and germination index behaviour during composting*.

826 **Table 5:** Chemical characteristics of composts obtained after 90 days of aerobic treatment [a] .
827

Table 1

Table 1: Thermal properties of PLA and PLA_20PBS based bionanocomposites.

Formulations	*DSC: First heating scan*								*Thermogravimetric analysis*	
	T_g (°C)	$\Delta H_{cc}(Jg^{-1})$	T_{cc}(°C)	$\Delta H_m(Jg^{-1})$	T_m(°C)	$\Delta H_m(Jg^{-1})$	T'_m(°C)	T''_m(°C)	T_{DI}(°C)	T_{DII}(°C)
PLA	47.2	19.5	98.0	-	-	24.6	147.1	153.6	364	-
Optimization of PBS content										
PLA_10PBS	46.3	6.2	76.5	6.6	111.5	23.7	143.5	153.6	363	393
PLA_20PBS	47.5	10.5	86.6	10.6	111.8	22.7	143.7	152.4	364	394
PLA_30PBS	47.6	12.0	90.7	16.9	112.2	20.4	141.8	153.2	363	395
Binary systems										
PLA_1CNC	46.9	26.3	99.2	-	-	28.3	145.4	153.6	364	-
PLA_3CNC	50.0	18.4	100.3	-	-	24.3	146.0	154.0	363	-
PLA_1s-CNC	47.9	17.4	85.1	-	-	28.3	141.6	152.7	351	-
PLA_3s-CNC	47.0	20.3	80.0	-	-	29.8	138.6	149.0	346	-
Ternary systems										
PLA_20PBS_1CNC	53.5	11.7	89.7	11.1	112.5	21.5	143.5	152.3	364	396
PLA_20PBS_3CNC	53.5	11.9	88.6	13.2	111.7	24.2	143.2	152.3	363	395
PLA_20PBS_1s-CNC	51.7	14.6	83.2	12.9	111.6	23.6	140.9	151.6	345	397
PLA_20PBS_3s-CNC	54.6	12.8	85.3	13.7	112.7	22.4	139.9	151.1	344	397

Table 2

Table 2: Mechanical properties of PLA and PLA_20PBS based systems.

Formulations	σ_y *(MPa)*	ε_y *(%)*	σ_B*(MPa)*	ε_B*(%)*	E_{Young} *(MPa)*
PLA	21.7 ± 4.2^{ab}	2.5 ± 0.7^{a}	32.7 ± 6.3^{d}	330 ± 50^{fg}	1250 ± 190^{bc}
PLA_1CNC	23.2 ± 5.4^{bc}	2.9 ± 0.7^{a}	26.8 ± 2.5^{cd}	275 ± 15^{de}	1300 ± 50^{cd}
PLA_3CNC	23.2 ± 2.1^{bc}	2.3 ± 0.2^{a}	22.7 ± 3.2^{bc}	160 ± 30^{a}	1540 ± 60^{e}
PLA_1s-CNC	21.5 ± 5.1^{ab}	2.6 ± 0.6^{a}	22.4 ± 3.9^{bc}	300 ± 30^{ef}	1400 ± 100^{de}
PLA_3s-CNC	22.9 ± 5.8^{bc}	2.6 ± 0.7^{a}	28.0 ± 4.8^{cd}	270 ± 20^{de}	1260 ± 75^{bcd}
PLA_20PBS	22.0 ± 4.7^{b}	3.7 ± 0.5^{b}	30 ± 5.0^{d}	360 ± 30^{g}	920 ± 30^{a}
PLA_PBS_1CNC	15.6 ± 3.8^{a}	4.2 ± 0.7^{b}	15.5 ± 2.2^{a}	210 ± 10^{b}	950 ± 50^{a}
PLA_PBS_3CNC	17.4 ± 4.7^{ab}	4.1 ± 1.3^{b}	21.4 ± 3.3^{ab}	230 ± 25^{bc}	1130 ± 90^{abc}
PLA_PBS_1s-CNC	19.9 ± 4.9^{ab}	3.9 ± 0.5^{b}	23.5 ± 4.1^{bc}	260 ± 25^{cd}	970 ± 20^{a}
PLA_PBS_3s-CNC	28.1 ± 2.2^{c}	4.0 ± 0.8^{b}	20.1 ± 1.6^{ab}	370 ± 40^{g}	1120 ± 75^{ab}

[a-g]Different superscripts within the same column indicate significant differences among formulations ($p<0.05$).

Table 3

Table 3: Barrier properties, internal transmittance (T_i) at 450 nm and gloss values at 60ºPLA_PBS based bionanocomposites formulations.

Formulations	***Barrier properties***			***Internal transmittance***	***Gloss Values***
	OP 10^{12}(cm^3 m^{-1} s^{-1} Pa^{-1})	***WVP (11-53%RH) (g mmkPa^{-1} h^{-1} m^{-2})***	***WVP (100-53%RH) (g mmkPa^{-1} h^{-1} m^{-2})***	***T_i(450nm)***	***Gloss 60°***
PLA	1.98±0.08^{g}	0.071 ±0.005^{a}	0.079 ±0.004^{de}	88.2±0.1^{e}	65.2±4.3^{f}
PLA_1CNC	1.66±0.06^{f}	0.060±0.002^{bc}	0.073 ±0.003^{cd}	88.1±0.2^{e}	56.0±3.7^{f}
PLA_3CNC	1.57±0.05^{ef}	0.061±0.005^{b}	0.087 ±0.013^{e}	87.8±0.1^{e}	48.9±2.2^{e}
PLA_1s-CNC	1.61±0.05^{ef}	0.055±0.001^{c}	0.087 ±0.013^{e}	87.9±0.1^{e}	81.5±1.6^{g}
PLA_3s-CNC	1.49±0.04^{de}	0.059±0.004^{bc}	0.068 ±0.002^{bc}	85.9±0.6^{d}	80.5±2.4^{g}
PLA_20PBS	1.35±0.02^{cd}	0.042±0.003^{d}	0.065 ±0.003^{bc}	86.0±0.1^{d}	35.1±3.6^{d}
PLA_20PBS_1CNC	1.26±0.01^{bc}	0.042±0.004^{d}	0.063 ±0.003^{ab}	85.5±0.1^{cd}	15.4±2.3^{b}
PLA_20PBS_3CNC	1.09±0.04^{ab}	0.041±0.001^{d}	0.071 ±0.008^{cd}	84.9±0.3^{b}	9.6±0.4^{a}
PLA_20PBS_1s-CNC	1.19±0.02^{abc}	0.040±0.002^{d}	0.055 ±0.005^{a}	85.0±0.2^{bc}	22.9±2.7^{c}
PLA_20PBS_3s-CNC	1.05±0.02^{a}	042±0.004^{d}	0.062 ±0.002^{ab}	81.2±0.6^{a}	20.9±0.4^{c}

$^{a-g}$Different superscripts within the same column indicate significant differences among formulations ($p<0.05$).

Table 4

Table 4: Organic matter loss, C/N ratio and germination index behavior during composting*.

	OM-loss (%)		*C/N*		*GI (%)*	
Time	***CNT compost***	***PLA_PBS compost***	***CNT compost***	***PLA_PBS compost***	***CNT compost***	***PLA_PBS compost***
StartingMixture	0.0		19.6		4.6 (1.9)	
20days	35.5	35.7	20.6	18.2	67.8 (10.8)	8.7 (4.4)
90days	36.2	43.4	18.6	24.4	66.5 (11.2)	78.6 (23.0)

*Values represent the mean expressed on a dry weight basis with standard error in brackets.

Table 5: Chemical characteristics of composts obtained after 90 days of aerobic treatment[a].

	CNT compost	***PLA_PBS compost***
Moisture (%)	64.7 (±0.3)	73.8 (±0.2)
pH	9.0 (±0.0)	8.7 (±0.0)
CE (dS m^{-1})	1.09 (±0.00)	0.82 (±0.00)
TOC (%)	29.7 (±0.5)	34.2 (±0.7)
TKN (%)	1.6 (±0.1)	1.4 (±0.1)
Organic N (% of total N)	78.0	84.8
TEC (%)	7.4 (±0.2)	6.3 (±0.2)
DH (%)	57.5	59.2
Total P (%)	0.5 (±0.1)	0.4 (±0.0)
Total K (%)	1.1 (±0.0)	1.1 (±0.0)
Total Cd (mg kg^{-1})	<0.02[b]	<0.02[b]
Total Cu (mg kg^{-1})	12.8 (±1.5)	12.2 (±0.2)
Total Hg (mg kg^{-1})	<0.05[b]	<0.05[b]
Total Ni (mg kg^{-1})	9.8 (±0.3)	12.5 (±1.0)
Total Pb (mg kg^{-1})	31.2 (±5.9)	27.7 (±1.2)
Total Zn (mg kg^{-1})	125.7 (±20.6)	148.0 (±2.9)

[a]Except for moisture and GI, all data are expressed on a dry weight basis; Valuesrepresent the mean with standard error in brackets.

[b] Limit of sensitivity of the method used.

Figure 1

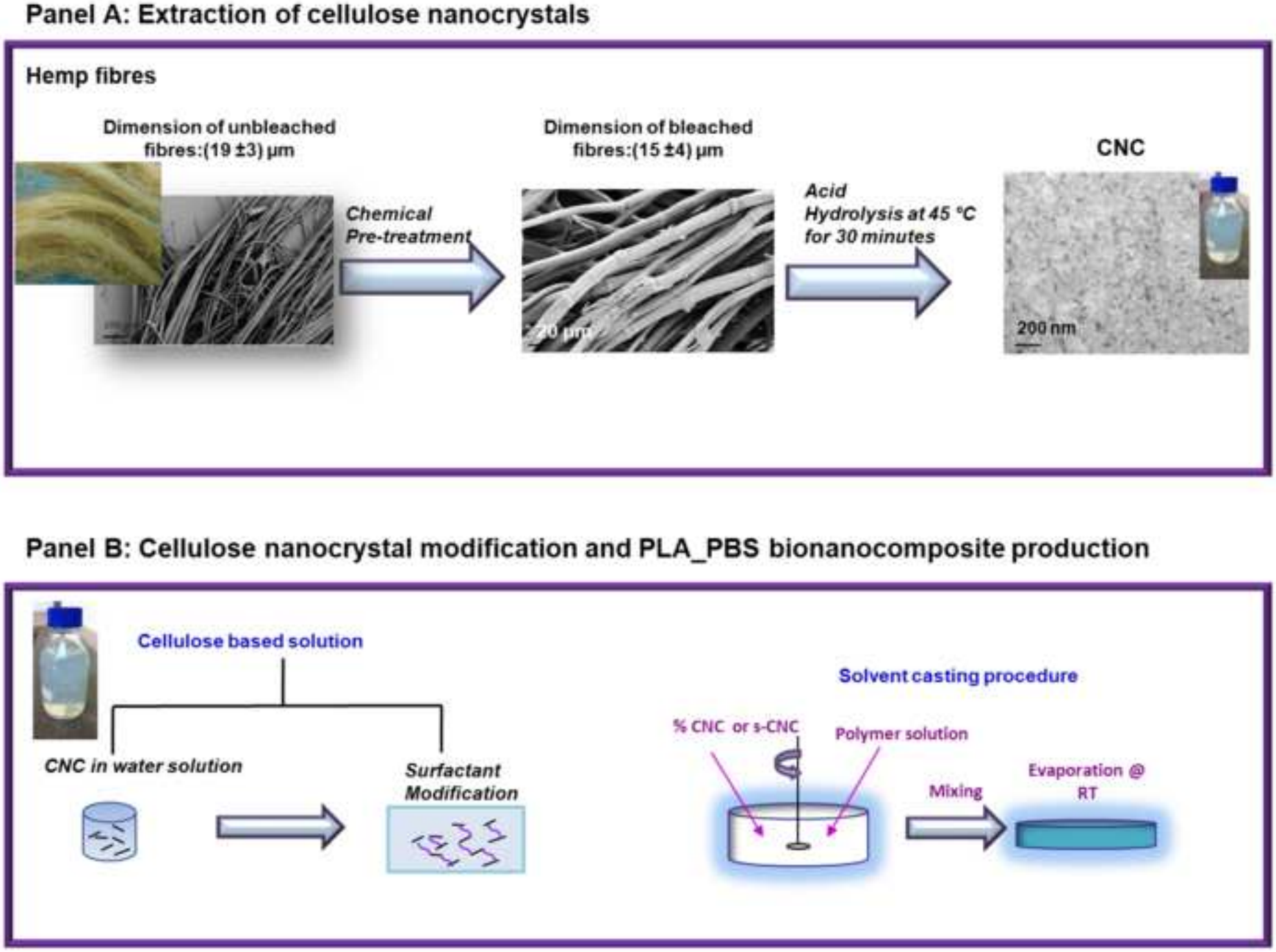
Panel A: Extraction of cellulose nanocrystals
Hemp fibres
Dimension of unbleached fibres:(19 ±3) µm
Chemical Pre-treatment
Dimension of bleached fibres:(15 ±4) µm
20 µm
Acid Hydrolysis at 45 °C for 30 minutes
CNC
200 nm
Panel B: Cellulose nanocrystal modification and PLA_PBS bionanocomposite production
Cellulose based solution
CNC in water solution
Surfactant Modification
Solvent casting procedure
% CNC or s-CNC
Polymer solution
Mixing
Evaporation @ RT

Figure 2

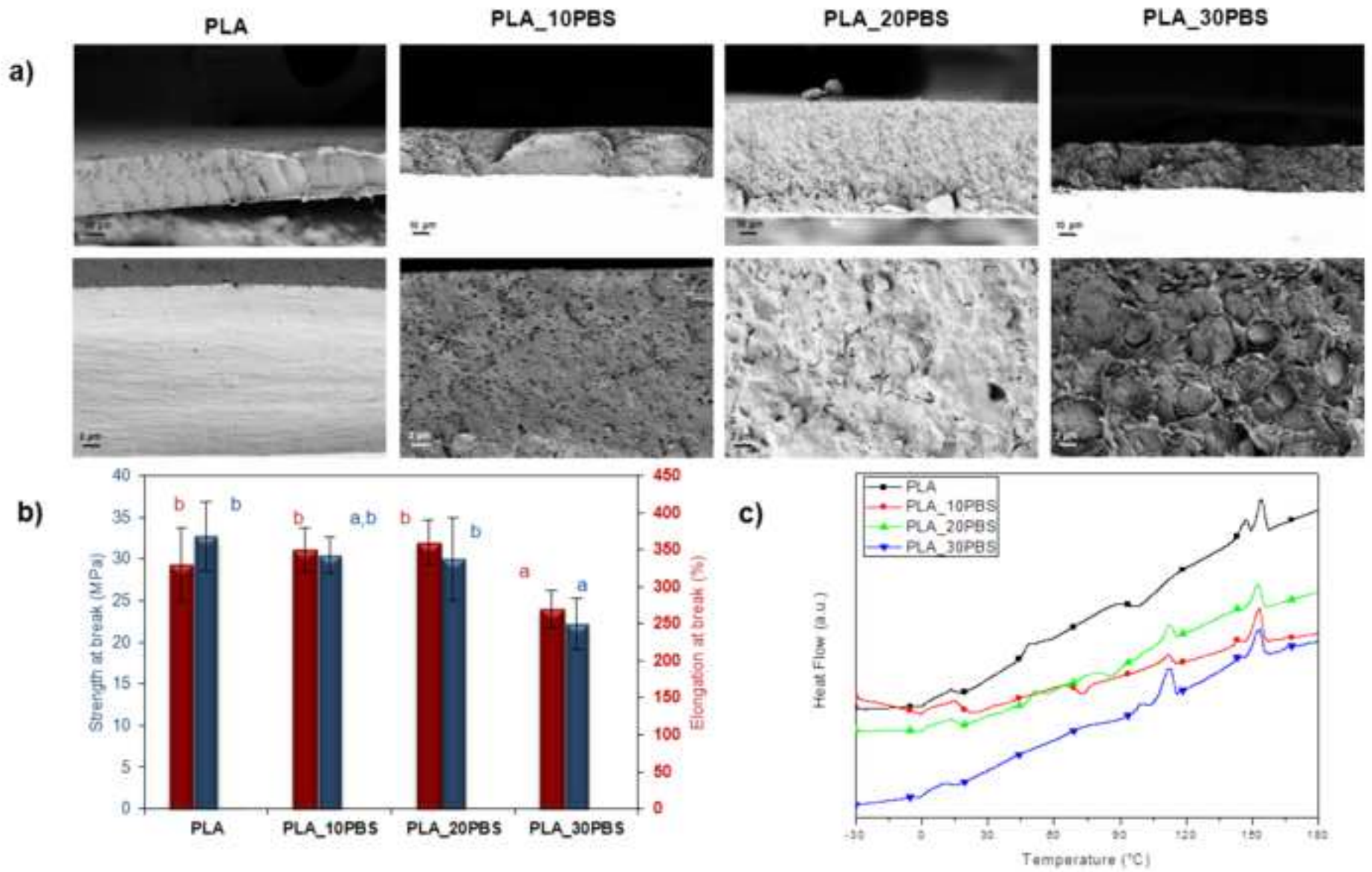
a)
PLA
PLA_10PBS
PLA_20PBS
PLA_30PBS
b)
Strength at break (MPa)
Elongation at break (%)
b
b
b
a,b
b
b
a
a
PLA
PLA_10PBS
PLA_20PBS
PLA_30PBS
c)
PLA
PLA_10PBS
PLA_20PBS
PLA_30PBS
Heat Flow (a.u.)
Temperature (°C)

Figure 3

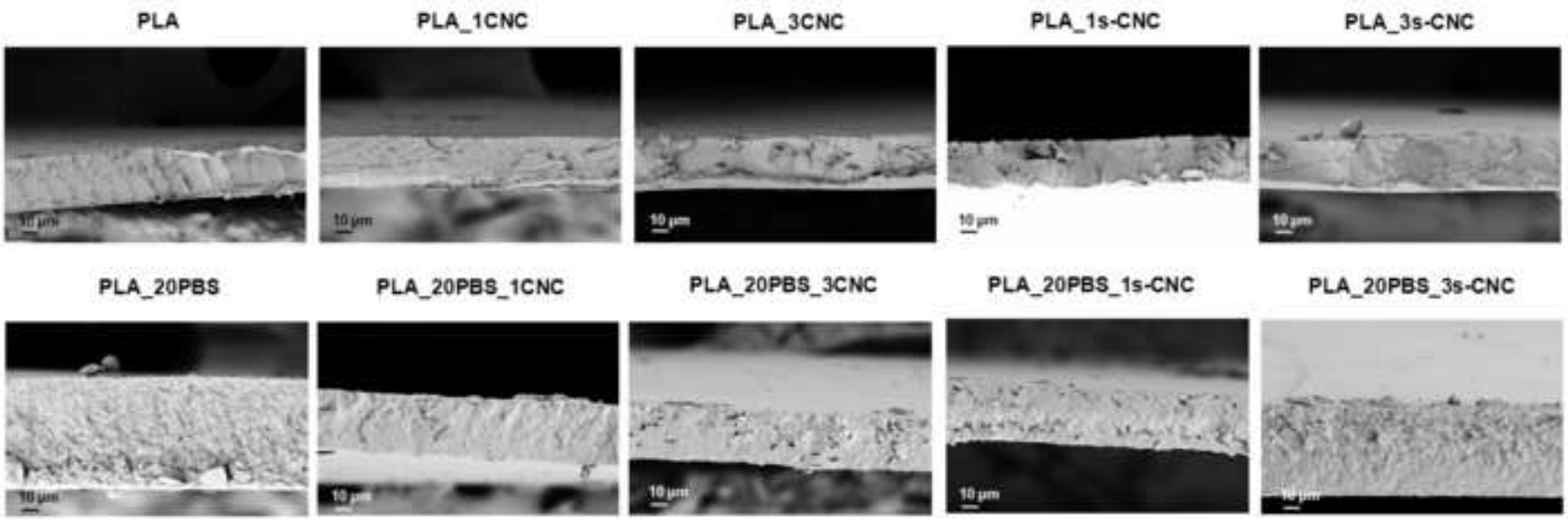
PLA
PLA_1CNC
PLA_3CNC
PLA_1s-CNC
PLA_3s-CNC
PLA_20PBS
PLA_20PBS_1CNC
PLA_20PBS_3CNC
PLA_20PBS_1s-CNC
PLA_20PBS_3s-CNC

Figure 4

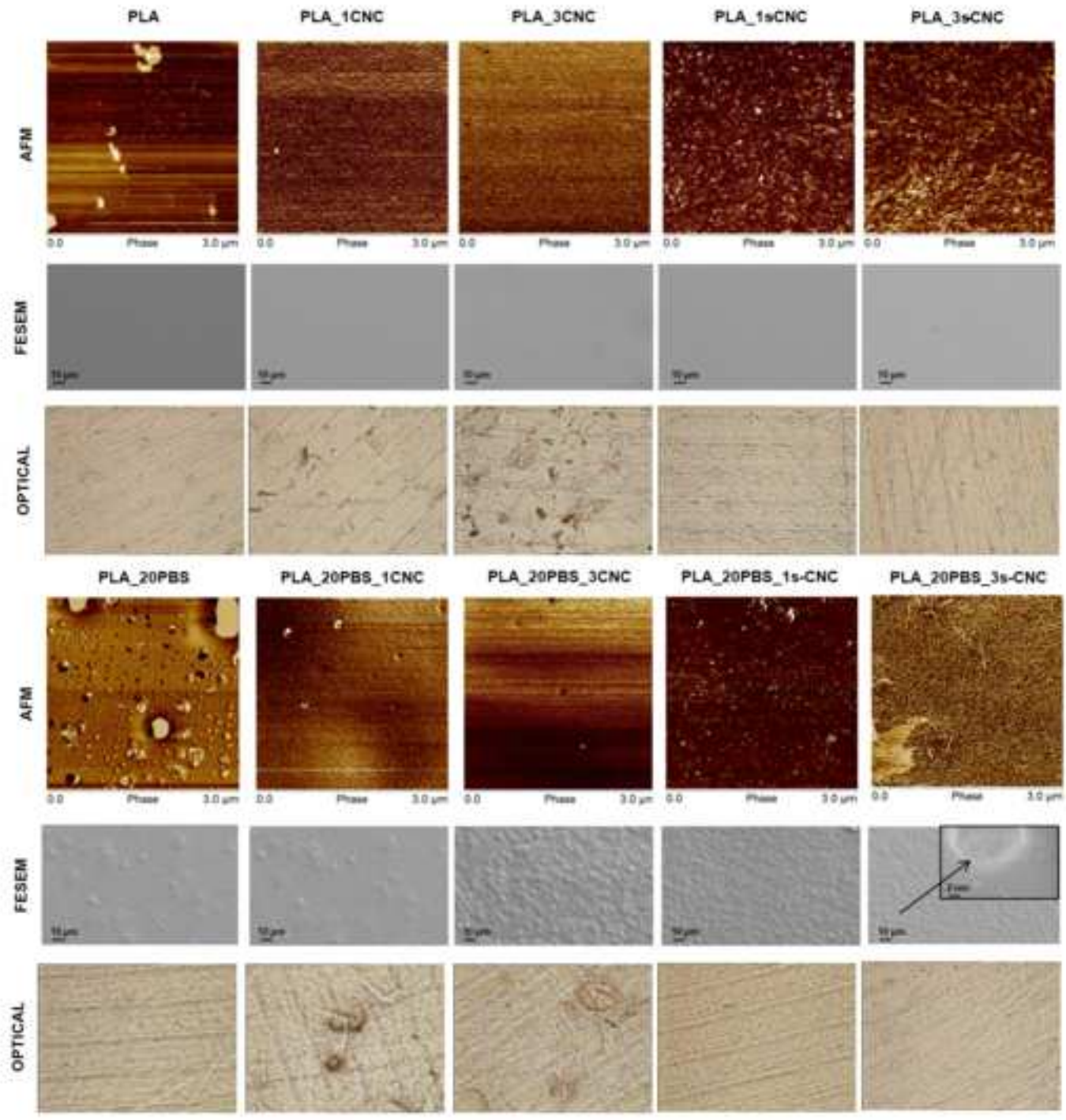
PLA
PLA_1CNC
PLA_3CNC
PLA_1sCNC
PLA_3sCNC
AFM
FESEM
OPTICAL
PLA_20PBS
PLA_20PBS_1CNC
PLA_20PBS_3CNC
PLA_20PBS_1s-CNC
PLA_20PBS_3s-CNC
AFM
FESEM
OPTICAL

Figure 5

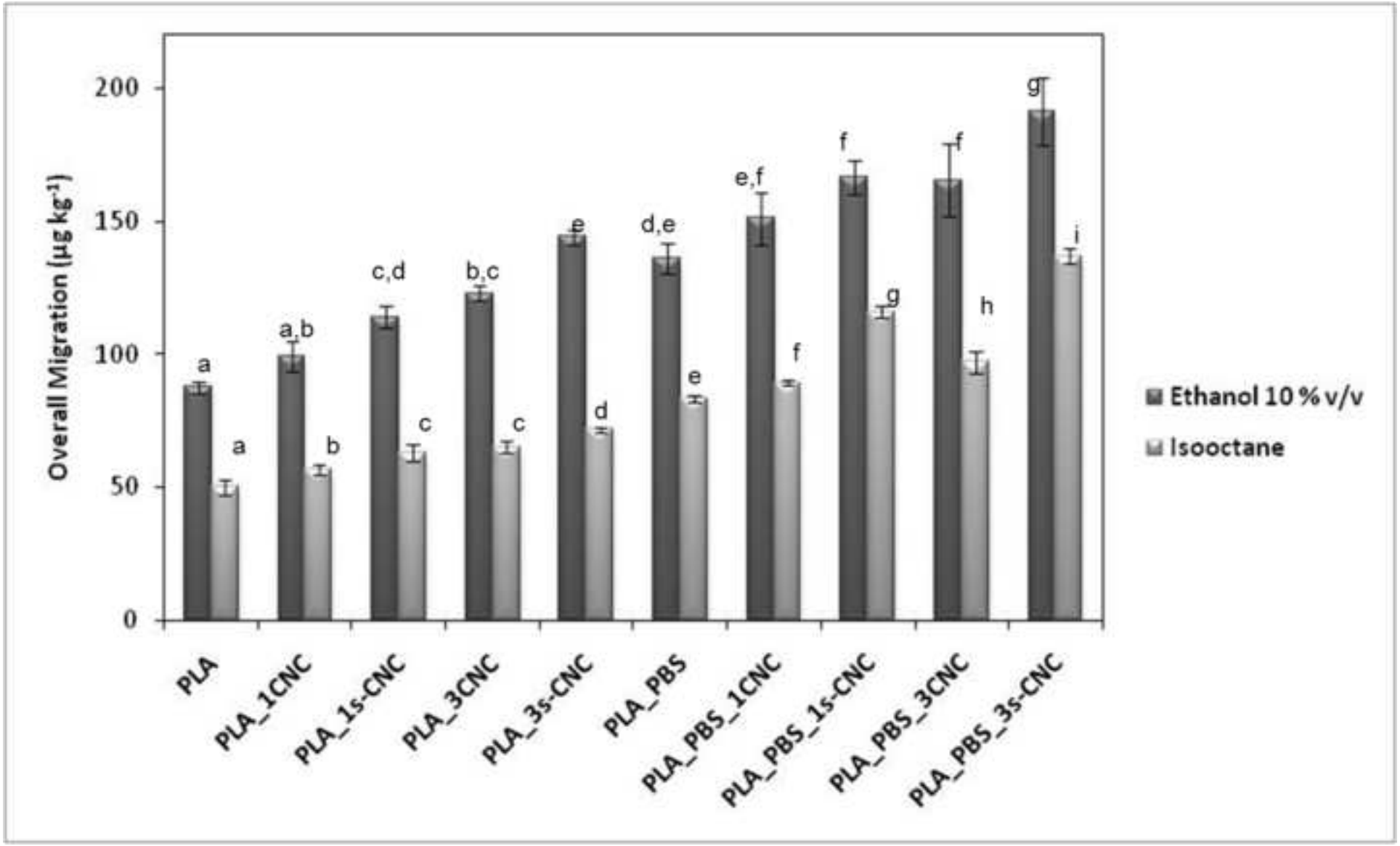
Overall Migration (µg kg-1)
200
150
100
50
0
a
a
a,b
b
c,d
c
b,c
c
e
d
d,e
e
e,f
f
f
g
f
h
g
i
PLA
PLA_1CNC
PLA_1s-CNC
PLA_3CNC
PLA_3s-CNC
PLA_PBS
PLA_PBS_1CNC
PLA_PBS_1s-CNC
PLA_PBS_3CNC
PLA_PBS_3s-CNC
Ethanol 10 % v/v
Isooctane

Figure 6

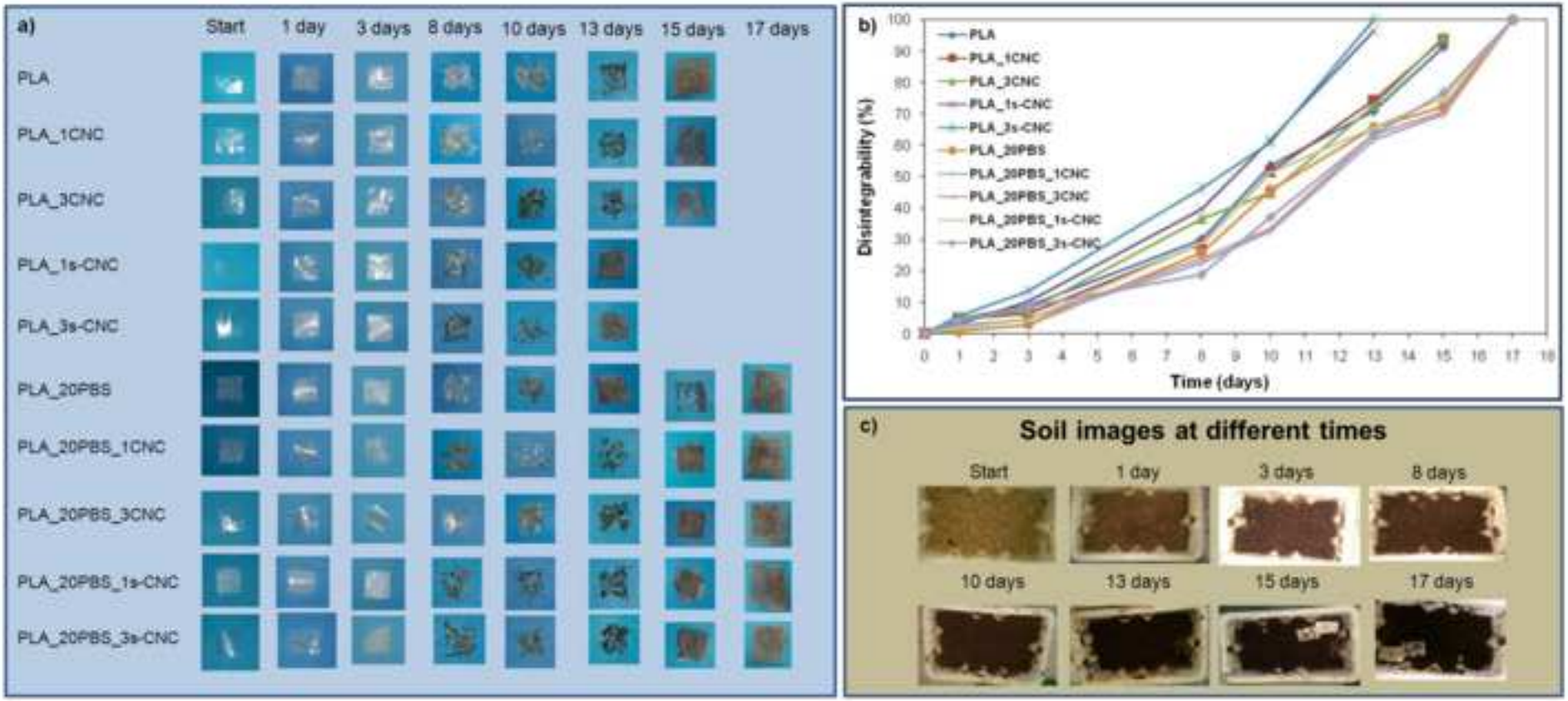
a)
Start
1 day
3 days
8 days
10 days
13 days
15 days
17 days
PLA
PLA_1CNC
PLA_3CNC
PLA_1s-CNC
PLA_3s-CNC
PLA_20PBS
PLA_20PBS_1CNC
PLA_20PBS_3CNC
PLA_20PBS_1s-CNC
PLA_20PBS_3s-CNC
b)
Disintegrability (%)
Time (days)
PLA
PLA_1CNC
PLA_3CNC
PLA_1s-CNC
PLA_3s-CNC
PLA_20PBS
PLA_20PBS_1CNC
PLA_20PBS_3CNC
PLA_20PBS_1s-CNC
PLA_20PBS_3s-CNC
c)
Soil images at different times
Start
1 day
3 days
8 days
10 days
13 days
15 days
17 days